

Challenges with interpreting the impact of Atlantic Multidecadal Variability using SST-restoring experiments

Christopher O'Reilly (✉ c.h.oreilly@reading.ac.uk)

University of Reading <https://orcid.org/0000-0002-8630-1650>

Matthew Patterson

University of Oxford

Jon Robson

University of Reading <https://orcid.org/0000-0002-3467-018X>

Paul Monerie

University of Reading

Dan Hodson

University of Reading <https://orcid.org/0000-0001-7159-6700>

Yohan Ruprich-Robert

Barcelona Supercomputing Center <https://orcid.org/0000-0002-4008-2026>

Article

Keywords:

Posted Date: June 6th, 2022

DOI: <https://doi.org/10.21203/rs.3.rs-1707393/v1>

License: © ⓘ This work is licensed under a Creative Commons Attribution 4.0 International License.

[Read Full License](#)

1 **Challenges with interpreting the impact of Atlantic Multidecadal Variability**
2 **using SST-restoring experiments**

3 Christopher H. O'Reilly,^a Matthew Patterson,^b Jon Robson,^c Paul Arthur Monerie,^c Daniel
4 Hodson,^c and Yohan Ruprich-Robert^d

5 ^a *Department of Meteorology, University of Reading, UK.*

6 ^b *Department of Physics, University of Oxford, UK.*

7 ^c *National Centre for Atmospheric Science, University of Reading, UK.*

8 ^d *Barcelona Supercomputing Center, Spain.*

9 *Corresponding author:* Christopher H. O'Reilly, c.h.oreilly@reading.ac.uk

10 ABSTRACT: Climate model simulations that restore SSTs in the North Atlantic have been used
11 to explore the climate impacts of Atlantic Multidecadal Variability (AMV). However, despite
12 simulations and observations exhibiting similar North Atlantic SST anomalies, experiments with
13 active SST-restoring in the Tropical North Atlantic exhibit strong positive surface heat-fluxes out of
14 the ocean with warm SST anomalies, which is not replicated in other simulations or observations.
15 The upward surface heat-fluxes that are systematically driven by the active SST-restoring in the
16 Tropical North Atlantic are found to be crucial for generating a strong local precipitation response
17 and the associated remote impact on the Pacific Walker circulation; these are both absent in other
18 simulations. The results of this study strongly suggest that experiments employing SST-restoring
19 (or prescribed SSTs) in the Tropical North Atlantic exaggerate the influence of the Atlantic on
20 patterns of global climate anomalies and its role in recent multidecadal SST trends.

Introduction

Over the past 150 years or so the observed variability of sea surface temperatures (SSTs) over the North Atlantic has exhibited substantial variability on multidecadal timescales, which is often referred to as the Atlantic Multidecadal Oscillation or Atlantic Multidecadal Variability (AMV; Delworth and Mann 2000; Enfield et al. 2001; Knight et al. 2005; Ting et al. 2009). The AMV has been linked to significant multidecadal variability in surrounding continental climate regions, including over North America (e.g. McCabe et al. 2004; Sutton and Hodson 2005; Hodson et al. 2010; Ting et al. 2011; Nigam et al. 2011; Ruprich-Robert et al. 2018; Zhang et al. 2019), Europe (e.g. Sutton and Hodson 2003; Sutton and Dong 2012; O'Reilly et al. 2017; Ghosh et al. 2017; Qasmi et al. 2020) and the Sahel (e.g. Folland et al. 1986; Zhang and Delworth 2006; Mohino et al. 2011; Martin et al. 2014). The AMV has also been linked to remote influences over the Pacific and East Asia (e.g. Lu et al. 2006; Zhang and Delworth 2007; Ruprich-Robert et al. 2017; Sun et al. 2017; Monerie et al. 2018, 2019). Understanding the influence of the North Atlantic on regional climate is therefore important for understanding and predicting climate variability.

Due to the relatively short observational record, many of the studies aiming to understand the impact of the AMV on regional climate variability have consisted of modelling studies to isolate and characterise the influence of the AMV. One common method is to prescribe SST boundary conditions in an atmospheric general circulation model and analyse the resulting climate influence of the AMV (e.g. Sutton and Hodson 2003, 2007; Wang et al. 2009; Simpkins et al. 2014). One drawback of using a prescribed SST boundary condition is that coupled ocean-atmosphere interactions are poorly represented and at any one location the ocean can act as an unrealistic source/sink of heat to the overlying atmosphere (e.g. Barsugli and Battisti 1998).

A relatively recent development that has been used to avoid the issues around prescribed SSTs has been the use of coupled models in which SSTs are nudged towards some target value. An example of these are *transient pacemaker experiments*, in which the temperatures in the upper-ocean mixed-layer are forced towards a prescribed and evolving temperature anomaly in a particular region (e.g. Kosaka and Xie 2013). A more idealised approach, which has been used to assess the impact of the AMV are *SST-restoring experiments* (referred to "idealised pacemaker experiments")

in some studies) in which SSTs are restored towards a time-invariant SST anomaly pattern across the North Atlantic (e.g. Boer et al. 2016; Ruprich-Robert et al. 2017; Meehl et al. 2021). The aim of these simulations is to determine the influence of the SST anomalies on the broader climate system without breaking the coupled interactions between the atmosphere and ocean and should therefore be superior to prescribing SSTs in an atmosphere-only simulation. Recent studies using SST-restoring simulations have demonstrated an important influence of the North Atlantic on the large-scale circulation over the North Atlantic sector but also remote influences over the Pacific and Asia. Perhaps the most striking impact of the AMV in these simulations is the influence on the Tropical Pacific and the further associated impacts (Li et al. 2016; Ruprich-Robert et al. 2017; Meehl et al. 2021; Ruprich-Robert et al. 2021; Trascasa-Castro et al. 2021; Yao et al. 2021; Hodson et al. 2022; Wang et al. 2022).

However, it is not clear that these SST-restoring experiments give an appropriate physical representation of the ocean-atmosphere interaction over the North Atlantic on decadal timescales. In this study we analyse the ocean-atmosphere interaction in SST-restoring simulations and demonstrate that, in some cases, they differ substantially from the behaviour seen in free-running coupled models and long observational/reanalysis datasets. These results have implications for interpreting the role of AMV on regional climate anomalies and global SST trend patterns in recent decades.

Results

SST and heat-flux relationships in SST-restoring experiments and free-running coupled models

In this section we analyse the SSTs and surface heat-fluxes associated with AMV in SST-restoring experiments, in which the SSTs are relaxed to a target AMV SST pattern, in free-running coupled model simulations (i.e. CMIP6 piControl and historical) and in observational datasets (see Methods). We begin our analysis by examining the differences (i.e. AMV positive minus AMV negative) between the SSTs in SST-restoring experiments (Figure 1). The IPSL and UM SST-restoring experiments generally show similar SST differences, particularly over the North Atlantic, in all the experiments. In the AMV and AMV-ExTrop experiments, the SST differences are significantly positive across the entire North Atlantic (Figure 1a,b,g,h), whereas in the AMV-

78 Trop experiments the positive differences are mostly limited to the subtropical region in which the
79 relaxation is applied (Figure 1d,e). The difference between the analogous positive and negative
80 periods in the free-running piControl simulations are similar across all three index regions over the
81 North Atlantic (Figure 1c,f,h) and are most similar to the AMV and AMV-Extrop SST-restoring
82 simulations. The differences in the free-running piControl simulations are also similar to the
83 observed SST anomaly pattern associated with the AMV, which are shown in Figure 1s (and is
84 similar for all regions and is also similar in the CMIP6 Historical simulations; Figure S2).

85 To examine how these SST anomalies interact with the atmosphere we now examine the differ-
86 ences in surface heat flux, Q . This is defined here as the net surface heat flux due to long and
87 shortwave radiative fluxes and latent and sensible turbulent heat fluxes with positive values being
88 out of the ocean. The surface heat flux differences between the positive and negative SST-restoring
89 experiments (Figure 1j-r) are generally positive in the regions in which the temperature anomalies
90 are being forced in the SST-restoring simulations: the surface heat flux differences are positive
91 over the whole North Atlantic in the AMV runs, positive over the tropical North Atlantic in the
92 AMV-Trop runs, and positive over the extratropical North Atlantic in the AMV-ExTrop runs. One
93 notable feature is the very different surface heat fluxes in the subtropical North Atlantic region in
94 the AMV and AMV-ExTrop simulations, positive in the AMV experiments and small and gener-
95 ally negative in the AMV-ExTrop experiments, this is despite exhibiting similar SST differences
96 in this region. In contrast to the SST-restoring experiments, the difference between the positive
97 and negative periods in the free-running piControl simulations are similar across all three index
98 regions and exhibit a pattern that most resembles the AMV-ExTrop SST-restoring experiments,
99 with positive values in the extra-tropics and negative values in the subtropics.

100 We can investigate the relationship between decadal SST and surface heat-flux anomalies in
101 more detail for midlatitude and subtropical North Atlantic regions by examining the scatter plots
102 shown in Figure 2. The equivalent decadal anomalies for the observational datasets are shown
103 by the black dots in Figure 1c,d,g,h. Here we examine the surface heat-flux anomalies but these
104 are dominated by turbulent heat-fluxes and similar results are found if only turbulent heat-flux
105 components are analysed (see Figures S3, S4, S6, S7). To compare across the different simulations
106 more directly, we computed linear regression coefficients between the surface heat-flux anomalies
107 (Q_{net}) and SST in the midlatitude and subtropical North Atlantic regions (shown in Figure 2i,j). The

108 regression coefficients were calculated in 140-year periods by randomly sampling decades from the
109 SST-restoring experiments and across all different ensemble periods/members in the free-running
110 piControl, Historical and AMIP-hist simulations.

111 In the midlatitude North Atlantic there is a positive relationship between the decadal SST and
112 surface heat flux anomalies in the SST-restoring experiments with active restoring (i.e. AMV &
113 AMV-ExTrop), in all the free running simulations and in the observations. The only exception
114 is the AMV-Trop experiment in the UM slab-ocean model, which has no active SST-restoring
115 in this region so SSTs respond passively to surface heat fluxes and the relationship is negative.
116 The regression coefficients are all broadly consistent with the observations in the free-running
117 models and AMV/AMV-ExTrop SST-restoring experiments; a notable exception is the AMIP-
118 hist simulation, which has an extremely strong positive relationship (see also the scatter plots in
119 Figure S5). As such, one can conclude that the systematic relationship between the decadal SST
120 and surface heat flux anomalies in the AMV and AMV-ExTrop experiments are similar to the
121 behaviour seen in observations and in free-running coupled models.

122 In the subtropical North Atlantic, however, there are major discrepancies between the SST-
123 restoring experiments with active restoring (i.e. AMV & AMV-Trop) and the observations and
124 free-running coupled models (Figure 2e,f,g,h). The AMV and AMV-Trop experiments both exhibit
125 systematically positive relationships between the decadal SST and surface heat flux anomalies in
126 the subtropical North Atlantic, in contrast to the observations and free running coupled model
127 simulations, which overall exhibit weakly negative relationships. This is particularly clear in the
128 regression plots (Figure 2j), where it is only the AMV, AMV-Trop and AMIP-hist experiments
129 that exhibit a positive heat-flux associated with positive SST anomalies in the subtropical North
130 Atlantic region, whereas the other simulations - including the AMV-ExTrop experiments - are
131 much more consistent with the relationship estimated for the observational datasets.

132 Overall, the AMV-ExTrop experiment, with SST-restoring in the extratropical North Atlantic
133 exhibits characteristics of ocean-atmosphere coupling on decadal timescales over the North Atlantic
134 that are consistent with free-running coupled models and observations. The AMV and AMV-Trop
135 experiments, in contrast, are not consistent with free-running coupled models and observations,
136 particularly in the subtropical North Atlantic region.

137 It is also of interest to examine the seasonal dependence of the SST/surface heat-flux relationships
 138 (shown in Figures S9 & S10). In the midlatitude region there is a positive relationship throughout
 139 most of the year in the AMV, AMV-ExTrop and free-running piControl and Historical simulations,
 140 with an increase at the start of the winter periods. This is not well constrained in the observational
 141 datasets but is reasonably consistent. In the subtropical region, the AMV and AMV-Trop SST-
 142 restoring experiments show positive SST/surface heat-flux relationships throughout the year; this
 143 is inconsistent with the AMV-ExTrop SST-restoring simulations and free-running piControl and
 144 Historical simulations, which show a positive relationship in the summer period and a negative
 145 relationship in the winter period. The seasonally varying SST/surface heat-flux relationship in the
 146 subtropical region is consistent with the observational estimates and is reminiscent of the response
 147 of the Tropical North Atlantic to wintertime El Nino event anomalies on seasonal timescales:
 148 SST anomalies are generated in winter by negative surface heat-flux anomalies and then damp
 149 to the atmosphere through positive surface heat-flux anomalies in the following summer (e.g.
 150 Alexander and Scott 2002). The seasonal dependence of the SST/surface heat-flux relationship
 151 show that the the AMV and AMV-Trop SST-restoring experiments are more consistent with the
 152 other experiments and observational data in the boreal summer season, when the positive SST
 153 anomalies drive upward surface heat-fluxes. This indicates that the behaviour seen in the AMV &
 154 AMV-Trop SST-restoring experiments is likely more realistic in the boreal summer season than in
 155 the boreal winter season.

156 **Links between the AMV and decadal precipitation anomalies**

157 Several studies exploring the remote influence of the AMV on the climate system have emphasised
 158 the influence of the SST anomalies on anomalous precipitation, ascent and associated divergence
 159 at upper levels (e.g. Meehl et al. 2021; Ruprich-Robert et al. 2021). The differences in precipitation
 160 rate between positive and negative SST periods in the SST-restoring experiments and analogous
 161 period are shown in Figure 3a-i. The warmer SSTs are associated with more precipitation across
 162 most of the the extra-tropics and the tropics in the North Atlantic. Particularly notable is the
 163 intensification of the Intertropical Convergence Zone (ITCZ) to the north of the equator in the
 164 Atlantic. Whilst the intensification of the precipitation in the Tropical North Atlantic region (shown
 165 by magenta box in Figure 3) is present in all experiments, it is much stronger in the AMV and

166 AMV-Trop experiments, in which there is active SST-restoring in the tropics. Comparison of the
167 precipitation strength in the Tropical North Atlantic region in the SST-restoring and free-running
168 ensembles, plotted in Figure 3j, indicates that the experiments with active SST-restoring (i.e.
169 AMV and AMV-Trop) can support substantially higher precipitation anomalies than in simulations
170 without active SST-restoring.

171 To examine the relationship between the SSTs and the precipitation in the Tropical North Atlantic
172 across the different simulations we computed linear regression coefficients between the decadal
173 anomalies (shown in Figure 3k). For the SST-restoring experiments, the precipitation response
174 to a given SST anomaly is substantially higher in the experiments with active SST-restoring (i.e.
175 AMV and AMV-Trop) than in simulations without active SST-restoring (i.e. AMV-ExTrop). An
176 interpretation consistent with this behaviour is that the SST-restoring acts as a constant source
177 of heat in the Tropical North Atlantic in this region, such that the positive surface heat-fluxes
178 (out of the ocean; c.f. Figures 1j,k,m,n & 2j) support more intense convection (and associated
179 heating) in the atmosphere of the Tropical North Atlantic. In the absence of active SST-restoring,
180 positive SST anomalies on average support increased precipitation in the Tropical North Atlantic,
181 however in the absence of restoring heat-flux there are no upward surface heat fluxes to support any
182 strong precipitation response. Similar results are found for an index of the inter-hemispheric SST
183 gradient (shown in Figure S11) with a higher sensitivity of precipitation to the inter-hemispheric
184 SST gradient found in the experiments with active SST-restoring (i.e. AMV and AMV-Trop).
185 Therefore, the SST-restoring in the Tropical North Atlantic seems crucial for driving the strong
186 positive surface heat-fluxes associated with warm SSTs, which is inconsistent with those seen
187 in free-running models and observational data, and that these positive surface heat-fluxes are
188 responsible for the stronger precipitation response seen in the SST-restoring experiments.

189 **Remote decadal links between the North Atlantic and Pacific**

190 To assess the remote influence of the AMV in the different experiments we now analyse the
191 large-scale atmospheric circulation anomalies in these experiments. We first focus on the influence
192 of the AMV on the Pacific Walker circulation, which has been highlighted in several previous
193 studies. The decadal Pacific walker circulation anomalies (defined as the SLP difference across
194 the Indo-Pacific region, following e.g. Vecchi et al. (2006)) are shown in Figure 4. For the

195 experiments with active SST-restoring in the Tropical North Atlantic, AMV & AMV-Trop, there
 196 is a significant strengthening of the Pacific Walker circulation on average, in response to the
 197 positive SST anomalies. The anomalous La Nina-like SST anomalies seen in the Tropical Pacific
 198 these simulations (i.e. Figure 1a,b,d,e) and in similar SST-restoring simulations are consistent
 199 with coupling to the strengthened Pacific Walker circulation and associated Trade winds (e.g.
 200 Meehl et al. 2021; Ruprich-Robert et al. 2021). In contrast, there are much weaker anomalies in
 201 the AMV-ExTrop experiments with no significant changes in either of the experiments. The free-
 202 running simulations systematically show the opposite link to the AMV, with positive SST anomalies
 203 associated with a weakening of the Pacific Walker circulation and El Nino-like SST anomalies in
 204 the Tropical Pacific (i.e. Figures 1c,f,i & S12, S13); there is no clear seasonal dependence on the
 205 sign of the response, though the changes are generally stronger during the boreal winter (Figure
 206 S14). This varies somewhat depending on the defined AMV region, however, overall it is evident
 207 that the strengthening of the Pacific Walker circulation in the AMV and AMV-Trop experiments is
 208 clearly not favoured in the free-running simulations, despite the presence of similar SST anomalies.

209 In the free-running coupled models, there is substantial spread in the relationship between SST
 210 and heat-flux in the subtropical North Atlantic (i.e. Figure 2g,h), indicating that decades with
 211 positive SST and surface heat-flux can occur despite not dominating the overall relationship (as in
 212 the AMV and AMV-Trop experiments). Therefore, it is of interest to examine the periods in the
 213 free-running simulations in which the SST and heat-flux are both positive or negative and compare
 214 these with the SST-restoring experiments. Composite differences between positive SST/heat-flux
 215 decades and negative SST/heat-flux decades in the subtropical North Atlantic (shown in Figure
 216 S15) reveal that, despite the positive heat-flux anomaly, there are El Nino-like SST anomalies in
 217 the Tropical Pacific and an anomalously weak Pacific Walker circulation, very similar to the full
 218 AMV differences (i.e. Figures 1c,f,i & S12, S13). Therefore, even when positive SSTs occur in
 219 conjunction with positive heat-fluxes in the free-running models they do not resemble to large-
 220 scale global patterns seen in the SST-restoring experiments and might instead be associated with
 221 variability local to the Tropical North Atlantic that does not influence the Tropical Pacific.

222 The strength of the response of the Tropical Pacific in the SST-restoring experiments has been
 223 linked to the injection of moist static energy into the upper troposphere through deep convection
 224 over the Tropical North Atlantic in the multi-model study by Ruprich-Robert et al. (2021). The

225 results presented here show the strongest precipitation anomalies over the Tropical North Atlantic
 226 in the AMV and AMV-Trop experiments are associated with a strengthening of the Pacific Walker
 227 circulation, whereas the weaker precipitation anomalies seen in the AMV-ExTrop and the free-
 228 running coupled simulations are not associated with any strengthening of the Pacific Walker
 229 circulation. In the AMV and AMV-Trop experiments the active SST-restoring in the subtropics
 230 seems to be essential to drive the strong positive surface heat-fluxes (from positive SST anomalies)
 231 in the subtropical North Atlantic; these are in turn responsible for driving the strongest precipitation
 232 anomalies and the remote response in the Tropical Pacific. The systematically positive surface
 233 heat-flux anomalies driving the precipitation anomalies are inconsistent with the behaviour seen in
 234 free-running coupled model simulations and also with the observational estimates, which suggests
 235 that the influence of the AMV on the Tropical Pacific is unrealistic in the AMV and AMV-Trop
 236 SST-restoring experiments.

237 **Examining the role of the Tropical Atlantic in recent multidecadal SST trends**

238 The use of SST-relaxation experiments has been used in the Tropical Atlantic region to examine
 239 the role of the the North Atlantic on global warming patterns. One notable study by Li et al.
 240 (2016) used experiments with SST-restoring in several regions and compared the responses to SST
 241 trends over recent decades and found that the SST-restoring over the Tropical Atlantic compared
 242 well with the observed warming pattern. Our analysis to this point indicates that SST-restoring
 243 in the Tropical Atlantic and the associated surface heat-fluxes may lead to unrealistic results, so
 244 in light of this it is of interest to re-visit the role of the Tropical Atlantic in recent trends. To do
 245 so we analyse two transient pacemaker experiments with SST-restoring in the North Atlantic and
 246 Tropical Pacific, respectively, as well as the corresponding CMIP6 historical simulations (all from
 247 the IPSL-CM6-LR climate model).

248 The observed SST trend over the period 1979-2012 (following Li et al. (2016)), along with the
 249 ensemble mean SST trends from the Historical , North Atlantic and Tropical Pacific pacemaker
 250 simulations, are shown in Figure 5a-d. The distinct SST trend pattern in the observations, with
 251 warming across the entire North Atlantic and cooling across much of the Tropical Pacific, is not
 252 replicated in either the Historical ensemble or the North Atlantic pacemaker ensemble, which
 253 both have warming across the Tropical and North Pacific. However, the observed SST trend

pattern in the the Tropical Pacific pacemaker ensemble is very similar to the observed SST trend across the Tropical Pacific and the North Atlantic. The importance of the Tropical Pacific for the trends over this period was previously demonstrated by Kosaka and Xie (2013), who found this was particularly important for the reduced rate of global warming during the "hiatus" period. The dissimilarity of the SST trends in the North Atlantic pacemaker ensemble and observations initially appears to contradict the results of Li et al. (2016). However, Li et al. (2016) did not use a transient pacemaker setup but instead used an idealised SST-restoring experiment forced towards an SST anomaly pattern matching the observed trend, very similar to the SST-restoring experiments analysed above. By scaling the IPSL SST-restoring AMV experiment (i.e. Figure 1a) to approximately match the magnitude of the observed trend over the North Atlantic - shown in Figure 5e - we recover the results of Li et al. (2016), with a global SST trend pattern that is similar to the observations.

So why are the AMV SST-restoring and North Atlantic pacemaker SST trends so different? To explore this we consider a simple toy-model of the SST anomaly in the subtropical North Atlantic (see Methods). The SST anomaly evolution and equivalent restoring heat-flux from integrating this toy-model are shown in in Figures 5f & 5g. Shown are results for two different experimental setup in the toy model: the first is a SST-restoring setup, which is the difference between two integrations - one targeting a positive anomaly and one targeting a negative anomaly; the second is a transient pacemaker setup that targets an evolving prescribed SST anomaly, as in the transient pacemaker experiment shown in Figure 5c. In these toy-model simulations the target SSTs are the observed SSTs in the case of the pacemaker and the constant equivalent trend in the case of the SST-restoring simulation (i.e. Figure 5e).

In the transient pacemaker toy model, the restoring heat-flux trend (1.6 Wm^{-2} per 34 yr) is around three times weaker than the constant restoring heat-flux (4.9 Wm^{-2}) in the SST-restoring toy model. This is in part because the SST in the Historical simulation exhibits a similar positive trend to the observations so less restoring heat-flux is required to follow the target temperature. In the proper SST-restoring experiments, the restoring heat-flux in the subtropics (i.e. AMV and AMV-Trop experiments) clearly drives anomalous surface heat-flux to the atmosphere (e.g. Figure 2). The scaled heat flux corresponding to the equivalent warming trend (i.e. Figure 5e) is about 6 Wm^{-2} , which is similar to the restoring heat-flux toy model (4.9 Wm^{-2}). In the North

Atlantic transient pacemaker experiment (i.e. Figure 5c), the subtropical surface heat-flux trend is $-1.2 \pm 2.9 \text{ Wm}^{-2}$ per 34 yr, which is not substantially different from zero and is consistent with the weak trend estimated from the toy model. Observational products show similarly negligible surface heat-flux trends over the subtropical North Atlantic region in recent decades (Cook and Vizzy 2020). In the transient pacemaker, the restoring heat-flux is seemingly very weak compared to internal variability (and possibly externally forced surface heat-flux variability) and therefore the positive surface heat-flux that is present in the constant SST-restoring experiment - which is crucial for generating the remote response in the Tropical Pacific - is not present in the North Atlantic pacemaker experiment and therefore exhibits a much weaker remote influence on the Pacific. The difference between the subtropical North Atlantic surface heat-flux in the transient pacemaker and the constant SST-restoring experiments can therefore explain the discrepancy in the pattern of the SST trends between these two approaches.

Discussion

In this study we have analysed the role of ocean-atmosphere interaction in the AMV and how this is represented in SST-restoring simulations, free-running coupled model simulations and observations. Whilst both SST-restoring simulations and free-running models exhibit broadly similar North Atlantic SST anomalies, the experiments with active SST-restoring in the Tropical North Atlantic exhibit strong positive surface heat-fluxes with warm SST anomalies. However, the other simulations, the AMV-ExTrop experiments and the free-running coupled models, as well as the limited observational data, demonstrate weakly negative surface heat-fluxes associated with warm SST anomalies in the subtropical North Atlantic. Moreover, the positive surface heat-fluxes driven by the active SST-restoring in the Tropical North Atlantic are found to be crucial for generating a strong precipitation response in the Tropical North Atlantic and the associated remote impact on the large-scale Pacific Walker circulation, which are both absent in the simulations without active SST-restoring and that more closely resemble the limited observational data. Our results suggest that previous studies that invoke the Tropical Atlantic as an important driver of the recent multidecadal SST trends in the Tropical Pacific likely exaggerate the influence of the Atlantic due to the incorrect sign of the surface heat fluxes in the experiments with active SST-restoring in the Tropical Atlantic.

To consider why the SST-restoring in the tropics leads to seemingly unrealistic results it is useful to revisit mechanisms that have been linked to North Atlantic SST anomalies in the literature. Studies using models and observations have shown that anomalous ocean heat flux convergence in the midlatitudes contributes to changes in the ocean heat content and associated SST anomalies (e.g. Knight et al. 2005; Robson et al. 2012; Zhang et al. 2019), linked to changes in the circulation of the horizontal gyres (e.g. Williams et al. 2014; Buckley et al. 2015) and the Atlantic Meridional Overturning Circulation (e.g. Zhang 2008; Moat et al. 2019). However, the SSTs in the subtropical branch of the AMV are typically more intermittent and are largely consistent with being forced by surface heat-fluxes (Li et al. 2020; Lai et al. 2022), with the basin-wide coherency resulting from a remote teleconnection from the midlatitudes and are amplified by local feedbacks that do not directly depend on ocean circulation (e.g. Xie 1999; Clement et al. 2015; Yuan et al. 2016; Oelsmann et al. 2020). In fully-coupled models and in available observational data, there are surface heat-flux out of the ocean in the midlatitudes (e.g. Gulev et al. 2013; O'Reilly et al. 2016; O'Reilly and Zanna 2018), consistent with ocean heat convergence in this region, whereas in the tropics the heat fluxes are weakly negative and into the ocean (e.g. Figure 1), consistent with being driven by atmospheric processes. The systematically strong upward subtropical surface heat-flux associated with the positive AMV in the AMV and AMV-Trop experiments is therefore seeming inconsistent with the mechanisms responsible for generating the AMV. As highlighted in the above analysis, periods in which there are upward surface heat-flux in the subtropical North Atlantic associated with positive SSTs do occur in the coupled models but these are associated with a weakening of the Pacific Walker circulation - the opposite of that seen in the SST-restoring experiments - and more likely reflect warm subtropical North Atlantic SST anomalies, driven by the Tropical Pacific changes, being damped to the atmosphere.

The results of this study strongly suggest that experiments employing SST-restoring (or prescribed SST boundary conditions) in the Tropical North Atlantic are likely to exaggerate the influence of SSTs in this region on global climate. In particular the remote impacts of the AMV in these experiments, such as those examined here and elsewhere showing the impact on Indo-Pacific SSTs (e.g. Li et al. 2016), rely strongly on the SST-restoring in the Tropical North Atlantic - this is an important result and mean that the results from these experiments should be treated with a degree of caution. The strong influence on the Tropical Pacific is particularly problematic because

changes in the SSTs here can themselves generate strong remote teleconnections. For example, a remarkable result in the multi-model study of Ruggieri et al. (2021) was that the most consistent feature of the extratropical circulation response to the AMV in SST-restoring experiments was the strong weakening of the Aleutian Low in the North Pacific, with less consistent response in the extratropical North Atlantic. However, the strong weakening of the Aleutian Low is only found when SST-restoring is applied in the Tropical North Atlantic (i.e. AMV and AMV-Trop, see Figure S11), which our study indicates has an unrealistic influence on the local and remote atmospheric response. It is worth highlighting that the use of SST-restoring or prescribed SSTs in the Tropical Atlantic to understand the influence of the North Atlantic has been used widely, with at least 75 published studies based on experiments using such approaches (see Supplementary Text for a non-exhaustive list). Our findings suggest that experimental setups that are more cautious with where the SST-restoring is applied, such as in the midlatitudes in AMV-ExTrop experiments or by applying the restoring seasonally where appropriate (i.e. the Tropical North Atlantic in boreal summer; Figures S9 & S10), would avoid exaggerating the influence of the Tropical Atlantic and be more suitable for understanding the role of AMV in the global climate system.

Methods

SST-restoring experiments

In this study we examine output from two models that both performed a full set of SST-restoring experiments, following the DCP-C experiments outlined in Boer et al. (2016). The first is the IPSL-CM6 fully-coupled ocean-atmosphere model ("IPSL SST-restoring" hereafter) and the second is the MetUM-GOML, which is the Global Ocean Mixed-Layer coupled configuration of the Met Office Unified Model ("UM SST-restoring" hereafter; Hiron et al. (2015)). In these SST-restoring experiments, the model SST is nudged towards either a positive or negative observed AMV anomaly pattern, over the following regions:

- *AMV*: The entire North Atlantic region (0-65°N; 80-0°W).
- *AMV-Trop*: The subtropical North Atlantic region (0-30°N; 80-0°W).
- *AMV-ExTrop*: The extratropical North Atlantic region (30-60°N; 80-0°W).

370 For the IPSL pacemaker experiments there are 25 ensemble members for both positive/negative
371 SST anomalies. For the UM pacemaker experiments there are 10 ensemble members for both posi-
372 tive/negative SST anomalies. All simulations last for 10-years. In the UM pacemaker experiments
373 the magnitude of the SST pattern is doubled to increase the signal to noise ratio (Monerie et al.
374 2019) - for this reason the IPSL results are shown with a different scaling (i.e. $\times 2$) on some of the
375 plots.

376 **Free-running climate model simulations**

377 We also use data from models simulations from the Coupled Model Intercomparison Project
378 6 (CMIP6) archive (Eyring et al. 2016). We analyse data from 318 different CMIP6 *Historical*
379 simulations (between 1870-2014, to match the HadISST observational dataset) from 33 different
380 models, totalling ≈ 46000 years of model data. We also analyse data from CMIP6 *piControl*
381 simulations from 16 different models, all of which have at least 250 years of data and several have
382 over 1000 years of data, totalling ≈ 11500 years of model data. For both Historical and piControl
383 simulations we chose to use all models that were available which had complete data for all the
384 variables required for the analysis in this study.

385 From the piControl simulations we define simple analogues to compare with the SST-restoring
386 simulations by calculating SST indices over the regions corresponding to the AMV, AMV-Trop and
387 AMV-ExTrop relaxation in the SST-restoring simulations (as defined above). For these analogues
388 we define a positive/negative decade as one in which the SST anomaly averaged over that region
389 exceeds a magnitude of 1 standard deviation (defined for each simulation separately, shown for the
390 AMV region in Figure S1). Whilst other papers have considered different definitions of the AMV
391 (or AMO in some studies), such as removing a global mean signal (e.g.), here we take the simplest
392 approach to most cleanly compare to the SST-restoring simulations. As a result, there appears to
393 be a global mean SST signal that appears in the piControl composites, possibly due to the aliasing
394 (or contribution) of the AMV to the global mean surface temperature that has been previously
395 documented in the CMIP6 piControl simulations (Parsons et al. 2020).

396 To complement the coupled model simulation we also use data from the AMIP-hist simulations
397 from the CMIP6 archive, which allow us to understand how the atmosphere responds to SSTs in
398 the absence of any oceanic response to the atmosphere. These simulations are an extended version

399 of the Atmospheric Model Intercomparison Project (AMIP) simulations forced with prescribed
400 observed SST boundary conditions over the period 1870-2014. We analyse data from 49 different
401 AMIP-hist simulations.

402 **Transient pacemaker experiments**

403 For the final part of the Results section we examine trends from two transient pacemaker exper-
404 iments using the IPSL-CM6 model. These simulations are the same as for the Historical CMIP6
405 simulations but with SSTs in (i) the North Atlantic and (ii) the Tropical Pacific, forced towards
406 an 12-month low-pass filtered temperature anomaly taken from observations following the DCPD
407 experimental protocol (Boer et al. 2016). These transient pacemaker experiments are different from
408 the SST-restoring experiments in that the the SST target pattern is constantly evolving, whereas the
409 target SSTs are fixed in the SST-restoring experiments. The transient pacemaker experiments also
410 have evolving external forcing (as in the Historical CMIP6 simulations), whereas the SST-restoring
411 experiments have fixed external forcing. Each of the transient pacemakers was performed with 10
412 ensemble members over the period 1920-2014.

413 **Observational datasets**

414 In addition to the model simulations we analyse observational SST data from the HadISST dataset
415 (Rayner et al. 2003), which is available from 1870. We use sea-level pressure (SLP) data from the
416 HadSLP2 dataset (Allan and Ansell 2006), which is a gridded dataset produced using a statistical
417 optimal interpolation method. We also use SLP and surface heat-flux data from the 20th Century
418 Reanalysis (20CR) v3 dataset (Compo et al. 2011; Slivinski et al. 2019), which is a reanalysis
419 dataset which only assimilates surface pressure observations and is forced by observed SSTs at the
420 lower boundary.

421 The heat-flux from the 20CR dataset should be treated with some caution because it is a derived
422 indirectly from the assimilating model rather than from direct observations (as in other reanalysis
423 products) and because the number of observations in the subtropical North Atlantic is substantially
424 less than in the midlatitudes. However, the constraint of the large-scale atmospheric circulation
425 at the surface and the SST boundary condition from below can provide useful constraints, as
426 demonstrated by comparison to direct observational estimates by (Gulev et al. 2013). The impact

of the assimilated observations can be estimated by comparing the 20CR results to those of from the AMIP-hist simulations (i.e. in Figure 2), which are in some ways similar to a reanalysis like but with the absence of any observational assimilation and merely forced by an prescribed SSTs from observations. In the Tropical North Atlantic the 20CR and AMIP-hist simulations behave quite differently, indicating that the assimilation of the in-situ surface pressure observations plays an important role in determining the behaviour seen in 20CR.

In the analysis here we focus on 10-year (or decadal) means, following the length of the SST-restoring simulations. The datasets from the CMIP6 models and observations were converted into non-overlapping 10-year means. All the model and observational dataset were interpolated to a common regular $5^\circ \times 5^\circ$ resolution grid. The historical and observational datasets were linearly detrended prior to the analysis to be consistent with previous studies (e.g. Gulev et al. 2013), however, the qualitative conclusions drawn here are not sensitive to this detrending.

Toy model of SST evolution

To analyse the influence of the SST-restoring heat-fluxes we use a simple toy-model of the SST anomaly, T' :

$$C \frac{\partial T'}{\partial t} = -\frac{C}{\tau_r}(T' - T'_{\text{target}}) - \frac{C}{\tau_{\text{clim}}}(T' - T'_{\text{clim}}), \quad (1)$$

where the first term on the r.h.s. is restoring heat-flux towards the target temperature anomaly on timescale $\tau_r = 60$ days (as in the SST-restoring experiments), the second term is a slower damping towards a background/climatological temperature on timescale $\tau_{\text{clim}} = 365$ days and C is the heat capacity of a mixed layer of depth 50m.

The model integrations in the text were performed by initialising the model at $T' = 0$ at the start of the integration in 1978. The model was then integrated forward until 2012 with a time-step of one day. For the SST-relaxation toy model runs, the T'_{target} was set to constant values of ± 0.4 with a background value of $T'_{\text{clim}} = 0$. The difference of these two runs was then calculated and is shown in Figure 5g. For the transient pacemaker toy-model runs, the T'_{target} was set to the 12-month low-pass filtered observed SST (from HadISST) in the subtropical North Atlantic region. The background value, T'_{clim} was set to the 12-month low-pass filtered (25-member) ensemble mean SST from the CMIP6 Historical simulations from the IPSL model. The SST-restoring heat-flux was taken as the right hand side of equation 1. The conclusions are not overly sensitive to the relaxation

455 timescales, with similar qualitative results found for $\tau_r < \tau_{\text{clim}}$, which is clearly justified based on
456 the clear impact of the SST-relaxation in the SST-restoring and transient pacemaker experiments.

457 **Significance testing and uncertainty estimates**

458 We estimate significance of the differences between positive and negative AMV composites (i.e.
459 Figure 1) using a Monte Carlo resampling in which the positive and negative subsets are combined
460 and then split into random subsets with the same numbers as the original subsets. The difference
461 of these random subsets is recorded and the process repeated 10000 times to give a measure of the
462 significance of the difference.

463 For the observational regression plots in Figure 2 we use a Monte Carlo phase randomisation
464 technique (e.g. Ebisuzaki 1997) which generates surrogate indices with the same spectral charac-
465 teristics (and therefore similar autocorrelation) as the AMV index being analysed. The regression
466 calculation is then repeated for 10000 random indices to give an estimate of the significance level.

467 **Data Availability Statement**

468 The model datasets used in this simulation are mostly available online from the CMIP6 archive.
469 The only exception is data used from the UM simulations, which is available from COR on request.
470 The observational datasets for SST, SLP and surface heat-fluxes are also all freely available online.

471 **Acknowledgements**

472 COR was supported by a Royal Society University Research Fellowship. MP was funded by
473 the EUCP project (Horizon 2020; Grant Agreement 776613). JR was funded by NERC via the
474 ACSIS program (NE/N018001/1) and via the WISHBONE project (NE/T013516/1). PAM was
475 funded by the EMERGENCE project under the Natural Environment Research Council (NERC
476 Grant NE/S004890/1) The project that gave rise to these results included YRR and received the
477 support of a fellowship from "la Caixa" Foundation (ID 100010434) and from the European
478 Union's Horizon 2020 research and innovation programme under the Marie Skłodowska-Curie
479 grant agreement No 847648 (fellowship code LCF/BQ/PR21/11840016).

480 **Author contributions**

481 COR conceived of the study and performed the analysis. All authors contributed to the analysis
482 of the results and the manuscript writing.

483 **Competing interests**

484 The authors declare no Competing Financial or Non-Financial Interests.

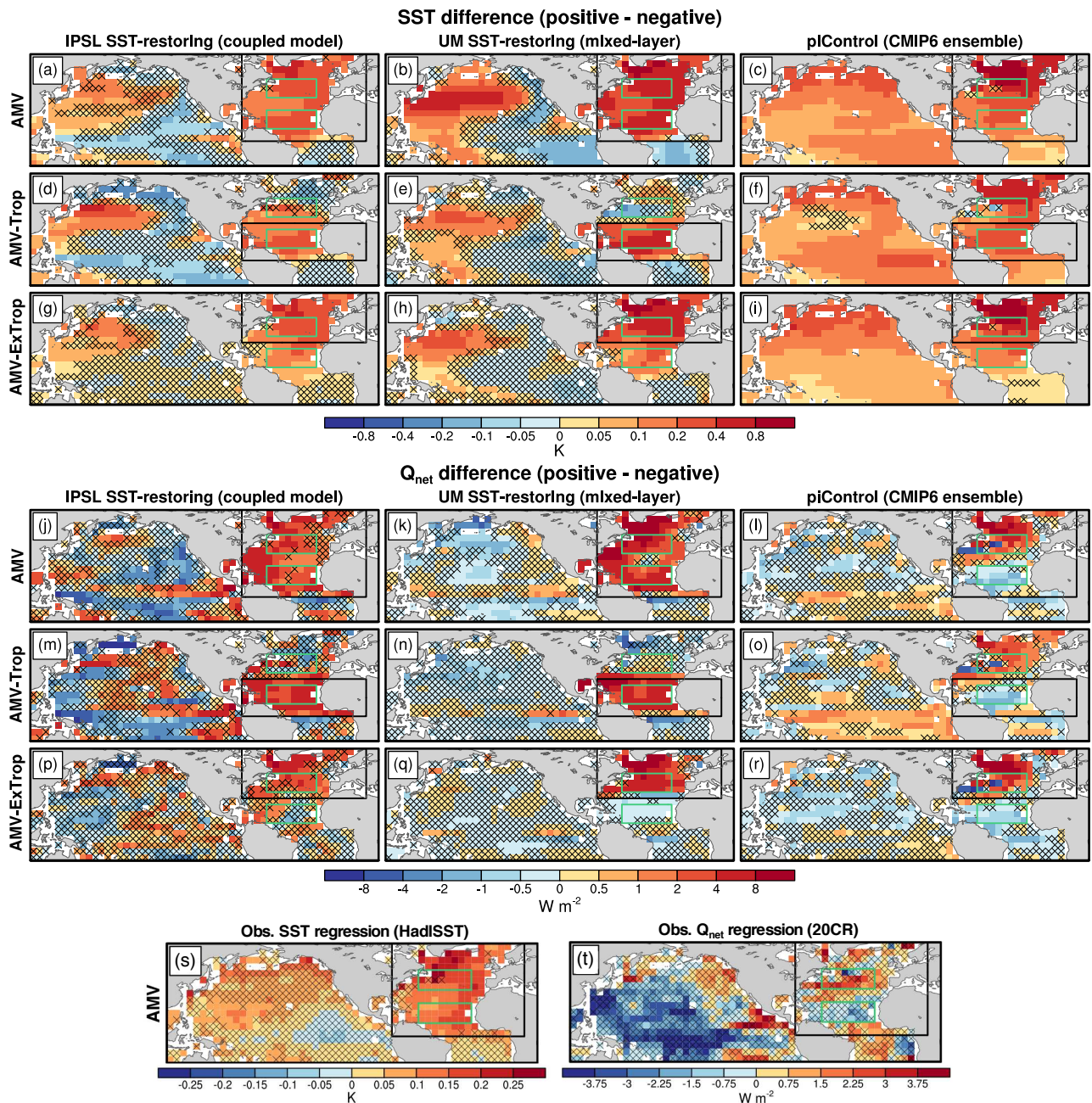
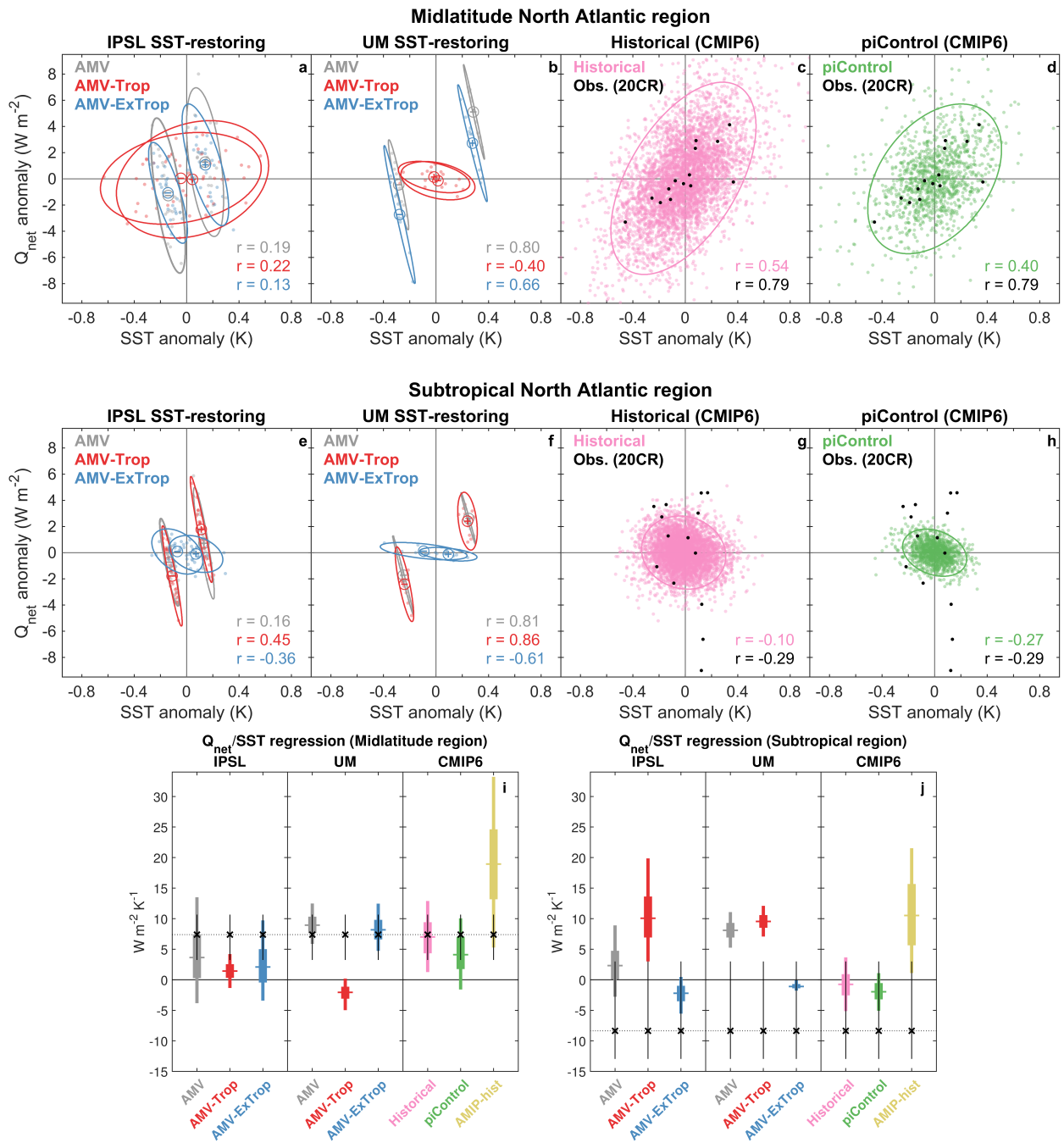


FIG. 1. (a-i) SST difference between SST+ and SST- 10-year periods for the AMV, AMV-Trop and AMV-ExTrop regions (indicated by the black boxes). These are shown for the SST-restoring experiments for the IPSL and UM models; for the free-running coupled PiControl simulations the SST+ and SST- decades are decades in which the SST in the region is above/below one standard deviation from the mean. (j-r) Surface heat-flux, Q_{net} (defined as positive upwards), difference between SST+ and SST- 10-year periods for the AMV, AMV-Trop and AMV-ExTrop regions. Hatching indicates where the differences are not significant at the 95% level, based on a Monte Carlo resampling performed 10000 times (see Methods). (s) Decadal SST anomalies (HadISST, 1870-2014) and (t) Q_{net} anomalies (20CR, 1870-2014) regressed onto a normalised decadal SST index averaged over the AMV region. Hatching in (s,t) indicates where the regression coefficients are not significant at the 95% level, based on a Monte Carlo phase randomisation test (see Methods).



495 FIG. 2. Scatter plots of decadal surface heat-flux (Q_{net}) anomalies (defined positive upwards) versus decadal
 496 SST anomalies over the midlatitude North Atlantic region (shown by green boxes in Figure 1) for (a) the idealised
 497 IPSL pacemaker experiments, (b) the idealised UM pacemaker experiments, (c) *Historical* simulations, and (d)
 498 *piControl* simulations. Each dot shows a value averaged over a different 10-year period and simulation and the
 499 ellipses show the two-dimensional Gaussian probability density function calculated across all the dots shown.
 500 The black dots show the decadal anomalies from the observational datasets (i.e. HadISST and 20CR). (e-h)
 501 As in (a-d) but for anomalies over the subtropical North Atlantic region (shown by green boxes in Figure 1).
 502 Also shown is the regression of decadal surface heat-flux anomalies onto decadal SST anomalies for (i) the
 503 midlatitude North Atlantic region and (j) the subtropical North Atlantic region. The regressions were calculated
 504 for all unique 140-year periods in the historical and piControl simulations and the box and whiskers show the
 505 5th-25th-50th-75th-95th percentiles of these distributions. For the SST-restoring experiments 10000 random
 506 140-year periods (i.e. 14 decades) were sampled and constructed from the ensemble members to calculate the
 507 regression; the box and whiskers show the distribution across these random samples for each experiment. The
 508 crosses and dotted lines show the equivalent regression coefficient calculated from the observational datasets.
 509 The vertical black lines are an estimate of the 5-95% confidence limits of the regression coefficient calculated
 510 from the observations, calculated using a block bootstrap resampling with replacement using a block length of
 511 20-years (repeated 10000 times).

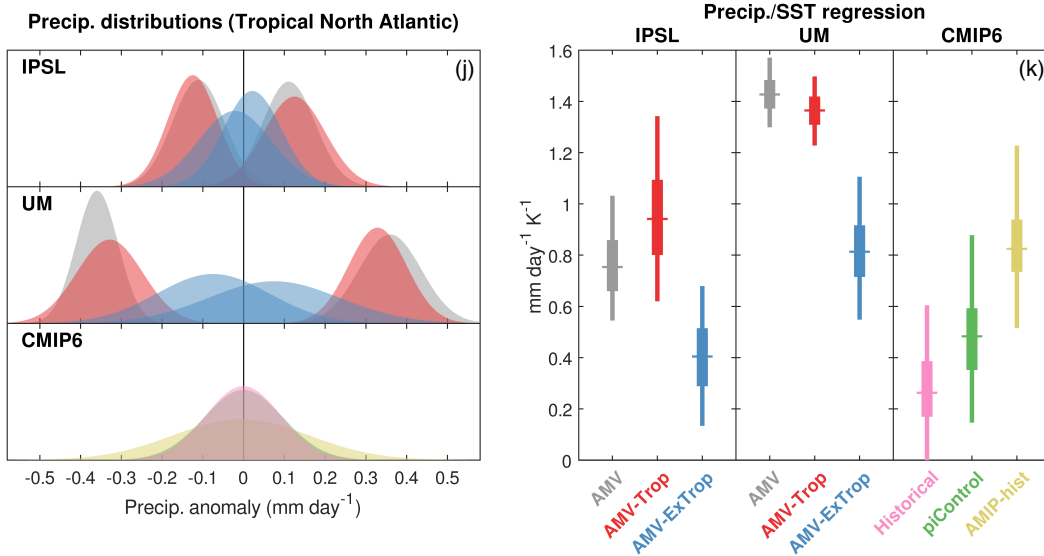
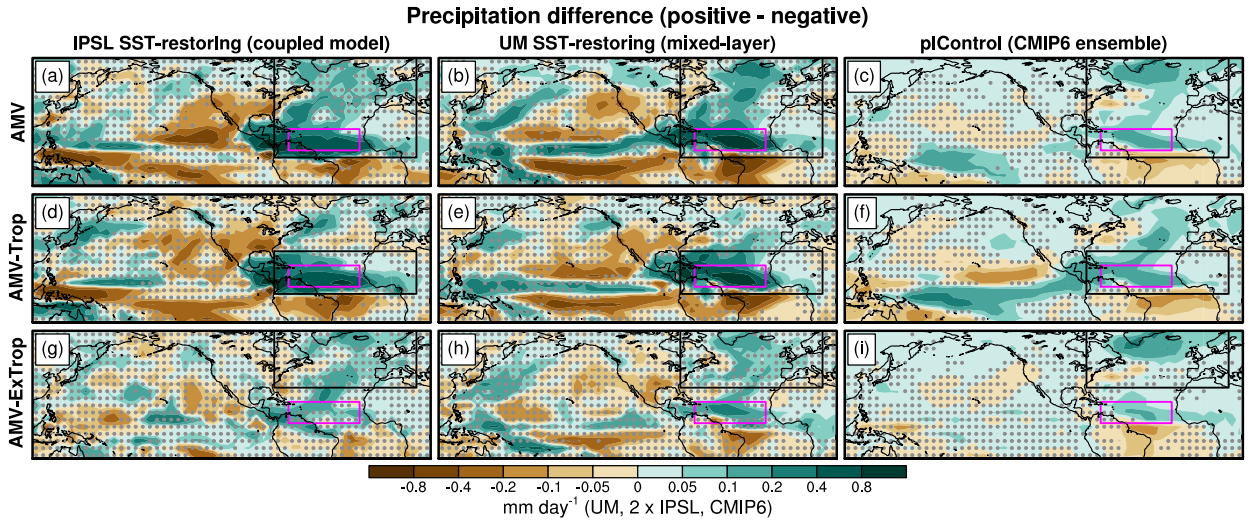


FIG. 3. (a-i) Precipitation difference between SST+ and SST- 10-year periods for the AMV, AMV-Trop and AMV-ExTrop regions (indicated by the black boxes). These are shown for the SST-restoring experiments for the IPSL and UM models; for the free-running coupled PiControl simulations the SST+ and SST- decades are decades in which the SST in the region is above/below one standard deviation from the mean. Hatching indicates where the differences are significant at the 95% level, based on a Monte Carlo resampling performed 10000 times (see Methods). (j) Gaussian distributions of the decadal tropical North Atlantic precipitation anomalies in the different ensembles (averaged over region shown in panels (a-i)). (k) Regression of decadal precipitation anomalies onto decadal SST anomalies for the subtropical North Atlantic region. The regressions were calculated for all unique 140-year periods in the historical and piControl simulations and the box and whiskers show the 5th-25th-50th-75th-95th percentiles of these distributions. For the SST-restoring experiments 10000 random 140-year periods (i.e. 14 decades) were sampled and constructed from the ensemble members to calculate the regression; the box and whiskers show the distribution across these random samples for each experiment.

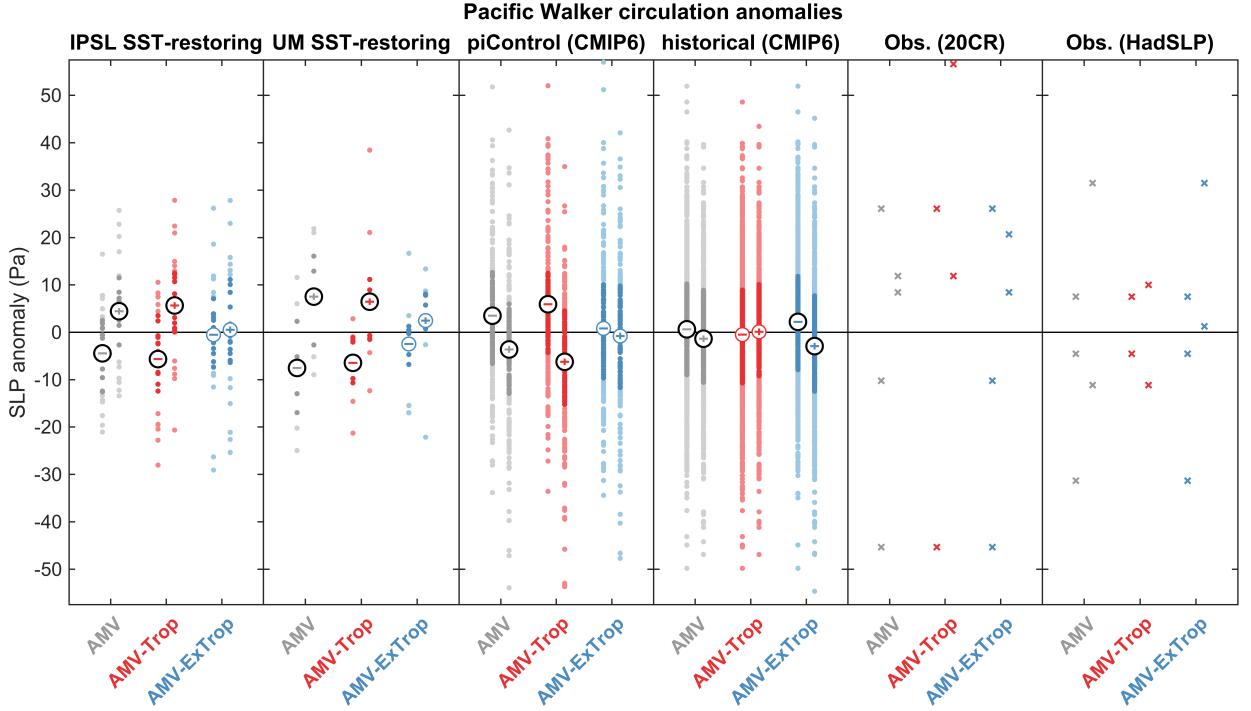


FIG. 4. Decadal Pacific Walker circulation anomalies for SST+ and SST- ensembles for the SST-restoring simulations. Also shown are the equivalent for the SST+ and SST- periods from the free-running historical and piControl CMIP6 simulations. Each dot indicates a single decadal period from one simulation, the darker shading indicates the interquartile range of the distributions and the circles with the "plus" and "minus" signs show the ensemble mean anomalies for the SST+ and SST- ensemble simulations, respectively. The circles surrounding the "plus" and "minus" signs are black and emboldened when the difference in the ensemble mean are significantly different at the 95% level based on a t-test. The equivalent data points are also shown for two observational datasets, 20CR and HadSLP2, with each decade shown by a cross.

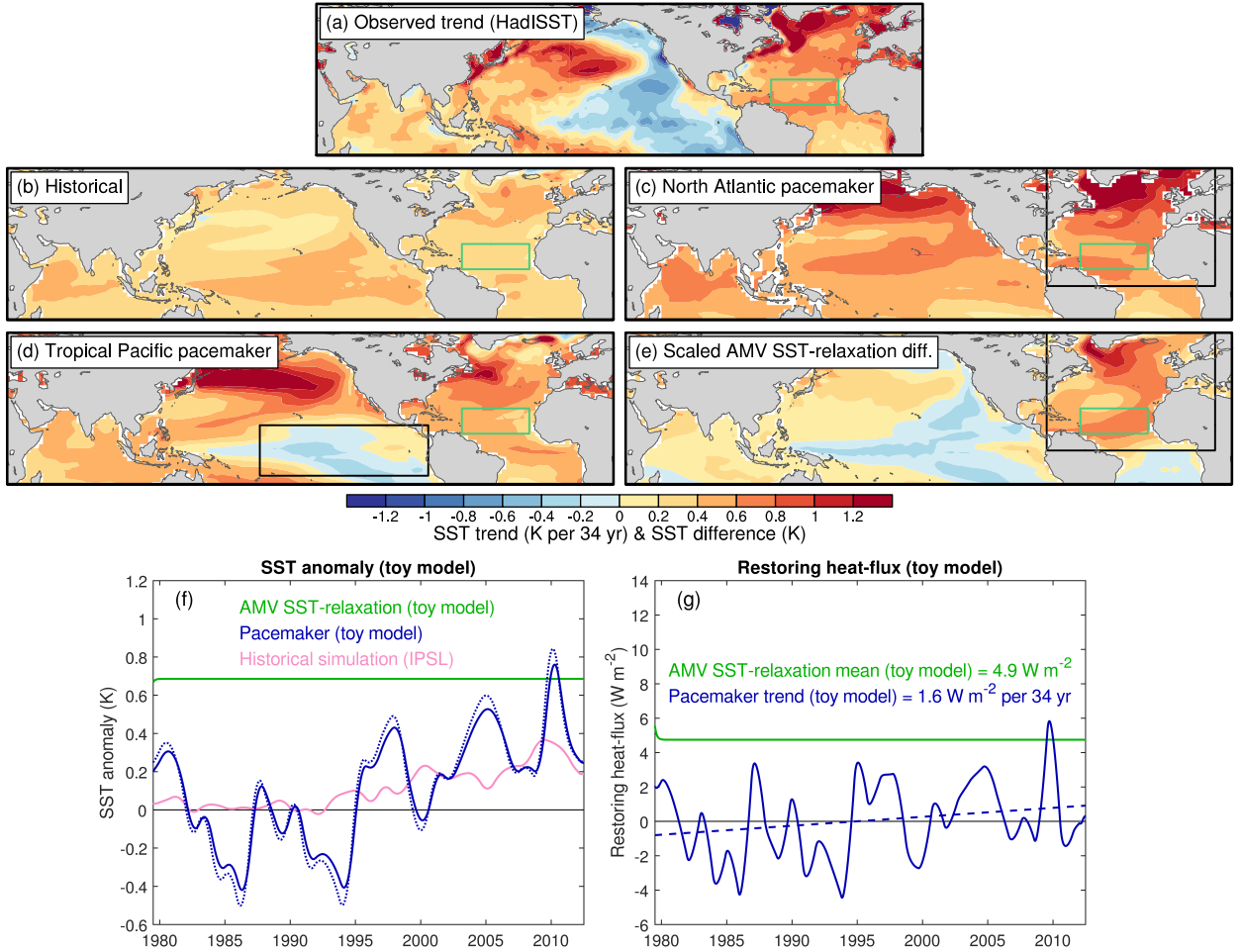


FIG. 5. SST trend over the period 1979-2012 in (a) observed SSTs from HadISST; (b) Historical IPSL ensemble mean; (c) North Atlantic IPSL pacemaker ensemble mean; (d) Tropical Pacific pacemaker ensemble mean; (e) Scaled IPSL SST-relaxation difference (i.e. scaled version of Figure 1a). (f) Subtropical SST anomaly evolution from the SST-restoring toy model discussed in the text (examining the trend and effective trend shown in panels (c) & (e)), shown for an idealised AMV SST-relaxation simulation, North Atlantic pacemaker, along with the ensemble mean subtropical SST anomaly from the IPSL historical simulation. (g) Restoring heat-flux evolution for the toy model simulations shown in (f); the dashed line shows the toy model pacemaker trend.

References

- Alexander, M., and J. Scott, 2002: The influence of ENSO on air-sea interaction in the Atlantic. *Geophysical Research Letters*, **29** (14), 46–1.
- Allan, R., and T. Ansell, 2006: A new globally complete monthly historical gridded mean sea level pressure dataset (HadSLP2): 1850–2004. *Journal of Climate*, **19** (22), 5816–5842.
- Barsugli, J. J., and D. S. Battisti, 1998: The basic effects of atmosphere–ocean thermal coupling on midlatitude variability. *Journal of the Atmospheric Sciences*, **55** (4), 477–493.
- Boer, G. J., and Coauthors, 2016: The decadal climate prediction project (DCPP) contribution to CMIP6. *Geoscientific Model Development*, **9** (10), 3751–3777.
- Buckley, M. W., R. M. Ponte, G. Forget, and P. Heimbach, 2015: Determining the origins of advective heat transport convergence variability in the North Atlantic. *Journal of Climate*, **28** (10), 3943–3956.
- Clement, A., K. Bellomo, L. N. Murphy, M. A. Cane, T. Mauritsen, G. Rädel, and B. Stevens, 2015: The Atlantic Multidecadal Oscillation without a role for ocean circulation. *Science*, **350** (6258), 320–324.
- Compo, G. P., and Coauthors, 2011: The twentieth century reanalysis project. *Quarterly Journal of the Royal Meteorological Society*, **137** (654), 1–28.
- Cook, K. H., and E. K. Vizy, 2020: Examining multidecadal trends in the surface heat balance over the tropical and subtropical oceans in atmospheric reanalyses. *International Journal of Climatology*, **40** (4), 2253–2269.
- Delworth, T. L., and M. E. Mann, 2000: Observed and simulated multidecadal variability in the Northern Hemisphere. *Climate Dynamics*, **16** (9), 661–676.
- Ebisuzaki, W., 1997: A method to estimate the statistical significance of a correlation when the data are serially correlated. *Journal of Climate*, **10** (9), 2147–2153.
- Enfield, D. B., A. M. Mestas-Núñez, and P. J. Trimble, 2001: The Atlantic multidecadal oscillation and its relation to rainfall and river flows in the continental US. *Geophysical Research Letters*, **28** (10), 2077–2080.

566 Eyring, V., S. Bony, G. A. Meehl, C. A. Senior, B. Stevens, R. J. Stouffer, and K. E. Taylor, 2016:
567 Overview of the Coupled Model Intercomparison Project Phase 6 (CMIP6) experimental design
568 and organization. *Geoscientific Model Development*, **9** (5), 1937–1958.

569 Folland, C. K., T. N. Palmer, and D. E. Parker, 1986: Sahel rainfall and worldwide sea temperatures,
570 1901–85. *Nature*, **320** (6063), 602–607.

571 Ghosh, R., W. A. Müller, J. Baehr, and J. Bader, 2017: Impact of observed North Atlantic
572 multidecadal variations to European summer climate: A linear baroclinic response to surface
573 heating. *Climate Dynamics*, **48** (11-12), 3547–3563.

574 Gulev, S. K., M. Latif, N. Keenlyside, W. Park, and K. P. Koltermann, 2013: North Atlantic Ocean
575 control on surface heat flux on multidecadal timescales. *Nature*, **499** (7459), 464–467.

576 Hirons, L., N. Klingaman, and S. Woolnough, 2015: MetUM-GOML1: a near-globally coupled
577 atmosphere–ocean-mixed-layer model. *Geoscientific Model Development*, **8** (2), 363–379.

578 Hodson, D. L., R. T. Sutton, C. Cassou, N. Keenlyside, Y. Okumura, and T. Zhou, 2010: Climate
579 impacts of recent multidecadal changes in Atlantic Ocean sea surface temperature: A multimodel
580 comparison. *Climate Dynamics*, **34** (7), 1041–1058.

581 Hodson, D. L., and Coauthors, 2022: Coupled climate response to Atlantic Multidecadal Variability
582 in a multi-model multi-resolution ensemble. *Climate Dynamics*, 1–32.

583 Knight, J. R., R. J. Allan, C. K. Folland, M. Vellinga, and M. E. Mann, 2005: A signature of
584 persistent natural thermohaline circulation cycles in observed climate. *Geophysical Research*
585 *Letters*, **32** (20).

586 Kosaka, Y., and S.-P. Xie, 2013: Recent global-warming hiatus tied to equatorial Pacific surface
587 cooling. *Nature*, **501** (7467), 403–407.

588 Lai, W., J. Robson, L. Wilcox, and N. Dunstone, 2022: Mechanisms of Internal Atlantic Mul-
589 tidecadal Variability in HadGEM3-GC3. 1 at Two Different Resolutions. *Journal of Climate*,
590 **35** (4), 1365–1383.

591 Li, L., M. S. Lozier, and M. W. Buckley, 2020: An investigation of the ocean’s role in Atlantic
592 multidecadal variability. *Journal of Climate*, **33** (8), 3019–3035.

Li, X., S.-P. Xie, S. T. Gille, and C. Yoo, 2016: Atlantic-induced pan-tropical climate change over the past three decades. *Nature Climate Change*, **6** (3), 275–279.

Lu, R., B. Dong, and H. Ding, 2006: Impact of the Atlantic Multidecadal Oscillation on the Asian summer monsoon. *Geophysical Research Letters*, **33** (24).

Martin, E. R., C. Thorncroft, and B. B. Booth, 2014: The multidecadal Atlantic SST—Sahel rainfall teleconnection in CMIP5 simulations. *Journal of Climate*, **27** (2), 784–806.

McCabe, G. J., M. A. Palecki, and J. L. Betancourt, 2004: Pacific and Atlantic Ocean influences on multidecadal drought frequency in the United States. *Proceedings of the National Academy of Sciences*, **101** (12), 4136–4141.

Meehl, G. A., and Coauthors, 2021: Atlantic and Pacific tropics connected by mutually interactive decadal-timescale processes. *Nature Geoscience*, **14** (1), 36–42.

Moat, B. I., and Coauthors, 2019: Insights into decadal North Atlantic sea surface temperature and ocean heat content variability from an eddy-permitting coupled climate model. *Journal of Climate*, **32** (18), 6137–6161.

Mohino, E., S. Janicot, and J. Bader, 2011: Sahel rainfall and decadal to multi-decadal sea surface temperature variability. *Climate dynamics*, **37** (3-4), 419–440.

Monerie, P., J. Robson, B. Dong, and Coauthors, 2019: Effect of the Atlantic multidecadal variability on the global monsoon. vol. 46. *Geophys Res Lett*, 1765–1775.

Monerie, P.-A., J. Robson, B. Dong, and N. Dunstone, 2018: A role of the Atlantic Ocean in predicting summer surface air temperature over North East Asia? *Climate Dynamics*, **51** (1), 473–491.

Nigam, S., B. Guan, and A. Ruiz-Barradas, 2011: Key role of the Atlantic multidecadal oscillation in 20th century drought and wet periods over the Great Plains. *Geophysical Research Letters*, **38** (16).

Oelsmann, J., L. Borchert, R. Hand, J. Baehr, and J. H. Jungclaus, 2020: Linking ocean forcing and atmospheric interactions to Atlantic multidecadal variability in MPI-ESM1. 2. *Geophysical Research Letters*, **47** (10), e2020GL087259.

620 O'Reilly, C. H., M. Huber, T. Woollings, and L. Zanna, 2016: The signature of low-frequency
621 oceanic forcing in the Atlantic Multidecadal Oscillation. *Geophysical Research Letters*, **43** (6),
622 2810–2818.

623 O'Reilly, C. H., and L. Zanna, 2018: The signature of oceanic processes in decadal extratropical
624 SST anomalies. *Geophysical Research Letters*, **45** (15), 7719–7730.

625 O'Reilly, C. H., T. Woollings, and L. Zanna, 2017: The dynamical influence of the Atlantic
626 Multidecadal Oscillation on continental climate. *Journal of Climate*, **30** (18), 7213–7230.

627 Parsons, L. A., M. K. Brennan, R. C. Wills, and C. Proistosescu, 2020: Magnitudes and spatial
628 patterns of interdecadal temperature variability in CMIP6. *Geophysical Research Letters*, **47** (7),
629 e2019GL086588.

630 Qasmi, S., C. Cassou, and J. Bo  , 2020: Teleconnection processes linking the intensity of the
631 Atlantic multidecadal variability to the climate impacts over Europe in boreal winter. *Journal of*
632 *Climate*, **33** (7), 2681–2700.

633 Rayner, N., D. E. Parker, E. Horton, C. K. Folland, L. V. Alexander, D. Rowell, E. C. Kent, and
634 A. Kaplan, 2003: Global analyses of sea surface temperature, sea ice, and night marine air
635 temperature since the late nineteenth century. *Journal of Geophysical Research: Atmospheres*,
636 **108** (D14).

637 Robson, J., R. Sutton, K. Lohmann, D. Smith, and M. D. Palmer, 2012: Causes of the rapid
638 warming of the North Atlantic Ocean in the mid-1990s. *Journal of Climate*, **25** (12), 4116–4134.

639 Ruggieri, P., and Coauthors, 2021: Atlantic multidecadal variability and North Atlantic jet: a
640 multimodel view from the decadal climate prediction project. *Journal of Climate*, **34** (1), 347–
641 360.

642 Ruprich-Robert, Y., T. Delworth, R. Msadek, F. Castruccio, S. Yeager, and G. Danabasoglu, 2018:
643 Impacts of the Atlantic multidecadal variability on North American summer climate and heat
644 waves. *Journal of Climate*, **31** (9), 3679–3700.

645 Ruprich-Robert, Y., R. Msadek, F. Castruccio, S. Yeager, T. Delworth, and G. Danabasoglu, 2017:
646 Assessing the climate impacts of the observed Atlantic multidecadal variability using the GFDL
647 CM2.1 and NCAR CESM1 global coupled models. *Journal of Climate*, **30** (8), 2785–2810.

648 Ruprich-Robert, Y., and Coauthors, 2021: Impacts of Atlantic multidecadal variability on the
649 tropical Pacific: a multi-model study. *npj climate and atmospheric science*, **4** (1), 1–11.

650 Simpkins, G. R., S. McGregor, A. S. Taschetto, L. M. Ciasto, and M. H. England, 2014: Tropical
651 connections to climatic change in the extratropical Southern Hemisphere: The role of Atlantic
652 SST trends. *Journal of climate*, **27** (13), 4923–4936.

653 Slivinski, L. C., and Coauthors, 2019: Towards a more reliable historical reanalysis: Improvements
654 for version 3 of the Twentieth Century Reanalysis system. *Quarterly Journal of the Royal
655 Meteorological Society*, **145** (724), 2876–2908.

656 Sun, C., F. Kucharski, J. Li, F.-F. Jin, I.-S. Kang, and R. Ding, 2017: Western tropical Pacific
657 multidecadal variability forced by the Atlantic multidecadal oscillation. *Nature communications*,
658 **8** (1), 1–10.

659 Sutton, R., and D. Hodson, 2003: Influence of the ocean on North Atlantic climate variability
660 1871–1999. *Journal of Climate*, **16** (20), 3296–3313.

661 Sutton, R. T., and B. Dong, 2012: Atlantic Ocean influence on a shift in European climate in the
662 1990s. *Nature Geoscience*, **5** (11), 788–792.

663 Sutton, R. T., and D. L. Hodson, 2005: Atlantic Ocean forcing of North American and European
664 summer climate. *science*, **309** (5731), 115–118.

665 Sutton, R. T., and D. L. Hodson, 2007: Climate response to basin-scale warming and cooling of
666 the North Atlantic Ocean. *Journal of Climate*, **20** (5), 891–907.

667 Ting, M., Y. Kushnir, R. Seager, and C. Li, 2009: Forced and internal twentieth-century SST trends
668 in the North Atlantic. *Journal of Climate*, **22** (6), 1469–1481.

669 Ting, M., Y. Kushnir, R. Seager, and C. Li, 2011: Robust features of Atlantic multi-decadal
670 variability and its climate impacts. *Geophysical Research Letters*, **38** (17).

671 Trascasa-Castro, P., Y. Ruprich-Robert, F. Castruccio, and A. C. Maycock, 2021: Warm phase
672 of AMV damps ENSO through weakened thermocline feedback. *Geophysical Research Letters*,
673 **48** (23), e2021GL096149.

- 674 Vecchi, G. A., B. J. Soden, A. T. Wittenberg, I. M. Held, A. Leetmaa, and M. J. Harrison, 2006:
675 Weakening of tropical Pacific atmospheric circulation due to anthropogenic forcing. *Nature*,
676 **441 (7089)**, 73–76.
- 677 Wang, C., B. Wang, L. Wu, and J.-J. Luo, 2022: A see-saw variability in tropical cyclone genesis
678 between the western North Pacific and the North Atlantic shaped by Atlantic multidecadal
679 variability. *Journal of Climate*, 1–37.
- 680 Wang, Y., S. Li, and D. Luo, 2009: Seasonal response of Asian monsoonal climate to the Atlantic
681 Multidecadal Oscillation. *Journal of Geophysical Research: Atmospheres*, **114 (D2)**.
- 682 Williams, R. G., V. Roussenov, D. Smith, and M. S. Lozier, 2014: Decadal evolution of ocean
683 thermal anomalies in the North Atlantic: The effects of Ekman, overturning, and horizontal
684 transport. *Journal of Climate*, **27 (2)**, 698–719.
- 685 Xie, S.-P., 1999: A dynamic ocean–atmosphere model of the tropical Atlantic decadal variability.
686 *Journal of Climate*, **12 (1)**, 64–70.
- 687 Yao, S.-L., W. Zhou, F.-F. Jin, and F. Zheng, 2021: North Atlantic as a Trigger for Pacific-Wide
688 Decadal Climate Change. *Geophysical Research Letters*, **48 (18)**, e2021GL094719.
- 689 Yuan, T., L. Oreopoulos, M. Zelinka, H. Yu, J. R. Norris, M. Chin, S. Platnick, and K. Meyer, 2016:
690 Positive low cloud and dust feedbacks amplify tropical North Atlantic Multidecadal Oscillation.
691 *Geophysical Research Letters*, **43 (3)**, 1349–1356.
- 692 Zhang, R., 2008: Coherent surface-subsurface fingerprint of the Atlantic meridional overturning
693 circulation. *Geophysical Research Letters*, **35 (20)**.
- 694 Zhang, R., and T. L. Delworth, 2006: Impact of Atlantic multidecadal oscillations on India/Sahel
695 rainfall and Atlantic hurricanes. *Geophysical research letters*, **33 (17)**.
- 696 Zhang, R., and T. L. Delworth, 2007: Impact of the Atlantic multidecadal oscillation on North
697 Pacific climate variability. *Geophysical Research Letters*, **34 (23)**.
- 698 Zhang, R., R. Sutton, G. Danabasoglu, Y.-O. Kwon, R. Marsh, S. G. Yeager, D. E. Amrhein, and
699 C. M. Little, 2019: A review of the role of the Atlantic meridional overturning circulation in

700 Atlantic multidecadal variability and associated climate impacts. *Reviews of Geophysics*, **57** (2),
701 316–375.

Supplementary Files

This is a list of supplementary files associated with this preprint. Click to download.

- [SuppInfov5.pdf](#)